Numerical simulation of salinity anomaly propagation in the Nordic seas and the Arctic Ocean

Rüdiger Gerdes & Cornelia Köberle

We investigate the response of the Nordic seas–Arctic Ocean system to surface freshwater flux anomalies that we regard as typical for long-term atmospheric variability. We employ response experiments with a coupled sea ice–ocean model where we introduce a surface freshwater flux anomaly (A) over the Norwegian Sea and (B) in the Laptev Sea. Case A offers an explanation for the intermediate depth salinity changes observed in the Amundsen Basin. The signal observed there belongs to an original perturbation that, according to the model, occurred around a decade earlier. Salinity fluctuations in the Laptev Sea could play a role in changes in the near surface salinity in the Amundsen Basin.

R. Gerdes & C. Köberle, Alfred Wegener Institute for Polar and Marine Research, Am Handelshafen 12, D-27570 Bremerhaven, Germany.

Introduction

Comparing results from two expeditions into the Eurasian Basin in 1991 and 1996, Schauer, Rudels et al. (unpubl. ms.) identified a warming from 1991 to 1996 in the core of the Atlantic Water at around 200 m and reduced salinity in a layer between 500 m and 1200 m deep in the Amundsen Basin. The latter is attributed to an increased outflow from the Barents Sea that feeds into a boundary current along the rim of the Eurasian Basin (Gerdes & Schauer 1997; Schauer, Muench et al. 1997). Schauer, Rudels et al. (unpubl. ms.) also confirm the disappearance – detected by Steele & Boyd (1998) – of the Arctic halocline in the central Eurasian Basin during recent years.

Model experiments are an important tool to investigate the relations between climate system components, their individual responses to external forcing, feedbacks, and internal modes of variability. Here we investigate the fate and possible influence of salinity anomalies that we regard as typical for long-term variability in the Nordic seas–Arctic Ocean system using a coupled sea ice–ocean model. In particular, we examine the response to (A) a precipitation anomaly over the Norwegian Sea that represents the main freshwater flux signal associated with the NAO according to Dickson et al. (in press) and (B) a freshwater flux anomaly in the Laptev Sea. The latter can be thought of as being generated by long-term wind anomalies associated with the NAO that influence sea ice formation and thus brine release in the Laptev Sea. Increased river run-off during periods of anomolously high precipitation over the catchment area would also lead to such a freshwater flux anomaly. Modelling these surface flux anomalies is not intended to investigate the response of the ocean to the NAO; this involves, among other variables, changes in the wind and air temperature. Here, we rather try to isolate the effect of a single element of the NAO forcing on sea ice and the ocean.

Model description and experimental design

The ocean model derives from the Geophysical Fluid Dynamics Laboratory modular ocean model (MOM-2; Pacanowski 1995). The model domain is shown in Fig. 1. Bottom topography is derived by horizontal averaging from the Etopo5 data set of the National Geophysical Data Center (1988). Modifications were made in Denmark Strait and the Faeroe Bank Channel area to retain the sill depths of the passages.

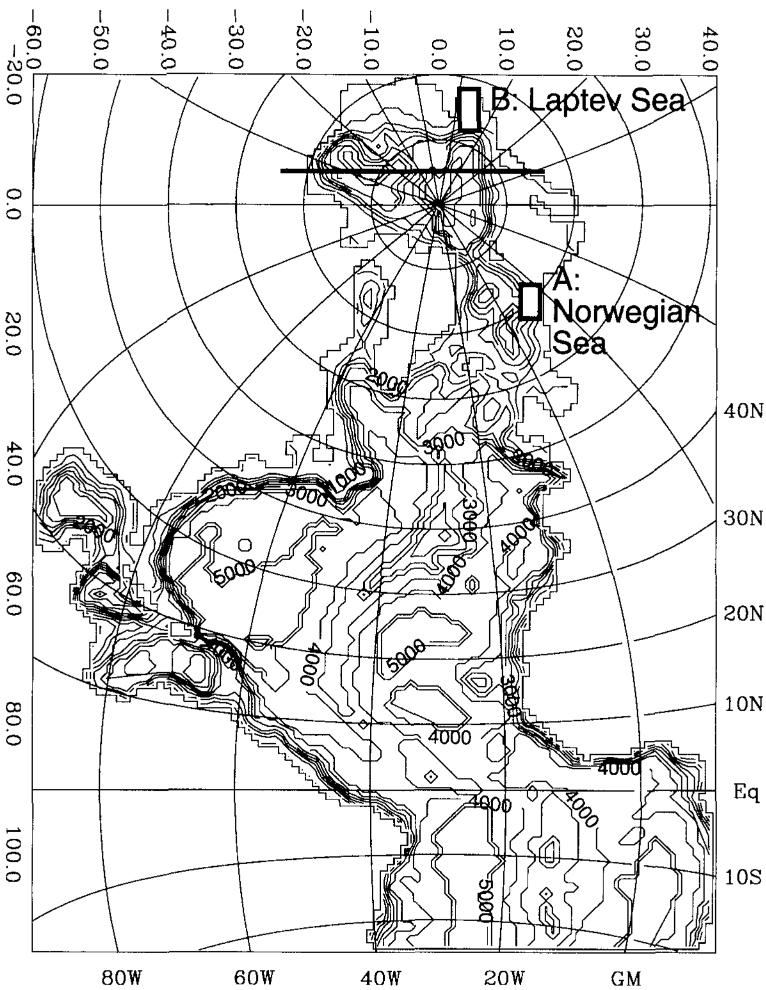

Fig. 1. Model domain and bottom topography for the numerical model used in this study. The model encompasses the Atlantic north of approximately 20°S, including the whole Arctic Ocean. The southern boundary is a closed wall. To avoid the singularity of geographical spherical coordinates at the pole the model is formulated on a rotated spherical grid where the equator coincides with the geographical 30°W meridian. The pole of the grid lies at 60°E on the geographical equator. The horizontal resolution is 1° by 1° in the rotated grid, resulting in nearly equal spacing of about 100 km in both horizontal directions in the whole Arctic Ocean. In the vertical, the model contains 19 unevenly spaced levels. The locations of freshwater flux anomalies are indicated for experiment A (off Norway) and B (Laptev Sea). The bold line along model longitude 5°W indicates the position of the section shown in Fig. 4.

The integration starts from rest and potential temperatures and salinities taken from Levitus & Boyer (1994a, b). North of 75°N initial data were taken from Levitus (1982) because of deficiencies of the newer climatology in the Arctic. The integration periods for experiments reported here are 20 years, 10 years of spin-up followed by a response experiment of equal length. Thermodynamic equilibrium is not reached and not intended for these numerical experiments. We have chosen this relatively short integration time so that the adjustment processes are modelled against a realistic background state, close to the climatological distributions that were used as initial conditions. The use of an additional tracer for salinity anomaly and a reference experiment without surface flux anomalies enables us to separate model drift and the response to forcing anomalies.

The ocean model is coupled with a dynamic–thermodynamic sea ice model that has been developed by Harder (1997) from the original Hibler (1979) model and employs a viscous-plastic rheology. The models are coupled following the procedure devised by Hibler & Bryan (1987).

Forcing data are derived from ECMWF data. Climatological monthly data are generated for surface air temperature, dew point temperature, cloudiness, precipitation and wind speed. These values are interpolated onto the current time in the model. Wind stress is treated similarly; however, here daily variability is added to make the simulation of sea ice more realistic. The procedure of generating the daily variability for a climatological mean year is described by Röske (in prep.). It should be noted that the climatology is based on the period 1979 to 1993. According to the nomenclature of Proshutinsky & Johnson (1997) this whole period (with the only exception of the years 1985 and 1987) belongs to the cyclonic circulation regime. The forcing is thus representative for the 80s and early 90s, and less so for earlier periods.

In addition to potential temperature and salinity, the ocean model carries another tracer representing the salinity anomaly. The tracer is initialized as zero everywhere and it obeys a no flux condition at the horizontal walls and the bottom. The no flux condition also applies at the surface except for the areas marked in Fig. 1: off Norway and in the Laptev Sea in experiments A and B, respectively. In experiment A a fresh water flux anomaly of 3 mm/day is switched on during three winter months (JFM) for three consecutive years following the 10 year spin-up. In experiment B we consider three consecutive winters with reduced sea ice formation of 1 m which represents a reduced salt flux into the ocean that is equivalent with an anomalous freshwater flux of 11 mm/day over the winter period. It should be noted that the salinity anomaly tracer is active in both experiments, i.e. it is added to the salinity before the equation of state is evaluated. A reference experiment without any anomalous surface freshwater fluxes accompanies the two response experiments and can be used to identify dynamical effects of the salinity anomalies like changes in surface density, currents and mixed layer depth.

Results

The distribution of salinity anomaly due to the higher precipitation in the Nordic seas (experiment A) in Fig. 2 shows the propagation from the source area into the Barents Sea and subsequently into the northern Kara Sea. As soon as the anomaly enters the Barents Sea, surface concentrations drop to less than 0.03 psu. Large northward velocities carry the induced salt anomaly out of the source area and no accumulation of freshwater occurs. Deep winter convection reaches the bottom in most parts of the Barents Sea and mixes the originally surface-trapped anomaly over a column 200–300 m thick. The dilution of the signal due to horizontal and vertical transports prevents a strong local density anomaly and the dynamical effect of the anomaly is small. The salt anomaly behaves like a passive tracer that is advected and mixed with the unaltered circulation and convection in the ocean.

A similar representation for the 300 m depth level (Fig. 3) shows the exit of the anomaly from the Barents Sea through the St. Anna Trough starting in the second year after the last anomalous winter precipitation off Norway. Small amounts of the anomaly appear west of the St. Anna Trough as a consequence of a direct inflow from Fram Strait. In the following years, the anomaly takes part in the cyclonic circulation around the Eurasian Basin and turns northward away from the boundary at the Lomonosov Ridge. It continues toward Fram Strait.

At greater depths, concentrations are lower and the inflow through Fram Strait gains relative importance. However, even at greater depths the outflow from the Barents Sea appears in the vicinity of the St. Anna Trough before the Fram Strait signal arrives at that location. The anomaly mainly follows the pathway of Barents Sea outflow as described by Schauer, Muench et al. (1997) and the numerical model of Gerdes & Schauer (1997). Because the outflow from the Barents Sea forms a thick layer in the Arctic, the salt anomaly is spread over a large vertical distance. The pathway is strongly affected by topographic structures, especially the Lomonosov Ridge. It takes about five years for the anomaly to reach the north pole.

A different picture emerges for the salinity anomaly in the Laptev Sea. Compared to the Norwegian Sea, the circulation in the Laptev Sea is slow. Thus in experiment B a large part of the accumulated freshwater remains in the Laptev Sea. Stratification is stable even during winter and no deep convection occurs, in contrast to conditions in the Barents Sea. Thus, surface salinity anomalies reach increasingly large values during the three anomalous winter conditions prescribed in experiment B. The surface salinity reaches 2 psu in the last year of the anomalous surface forcing (Fig. 4). It spreads into the interior of the Arctic Ocean along the oceanic transpolar drift (to be distinguished from the sea ice transpolar drift that presents a more direct connection to Fram Strait). The interior low salinity signal establishes within one year. Concentrations there reach 0.4 psu before the anomaly vanishes again after the cessation of the supply from the Laptev Sea. The

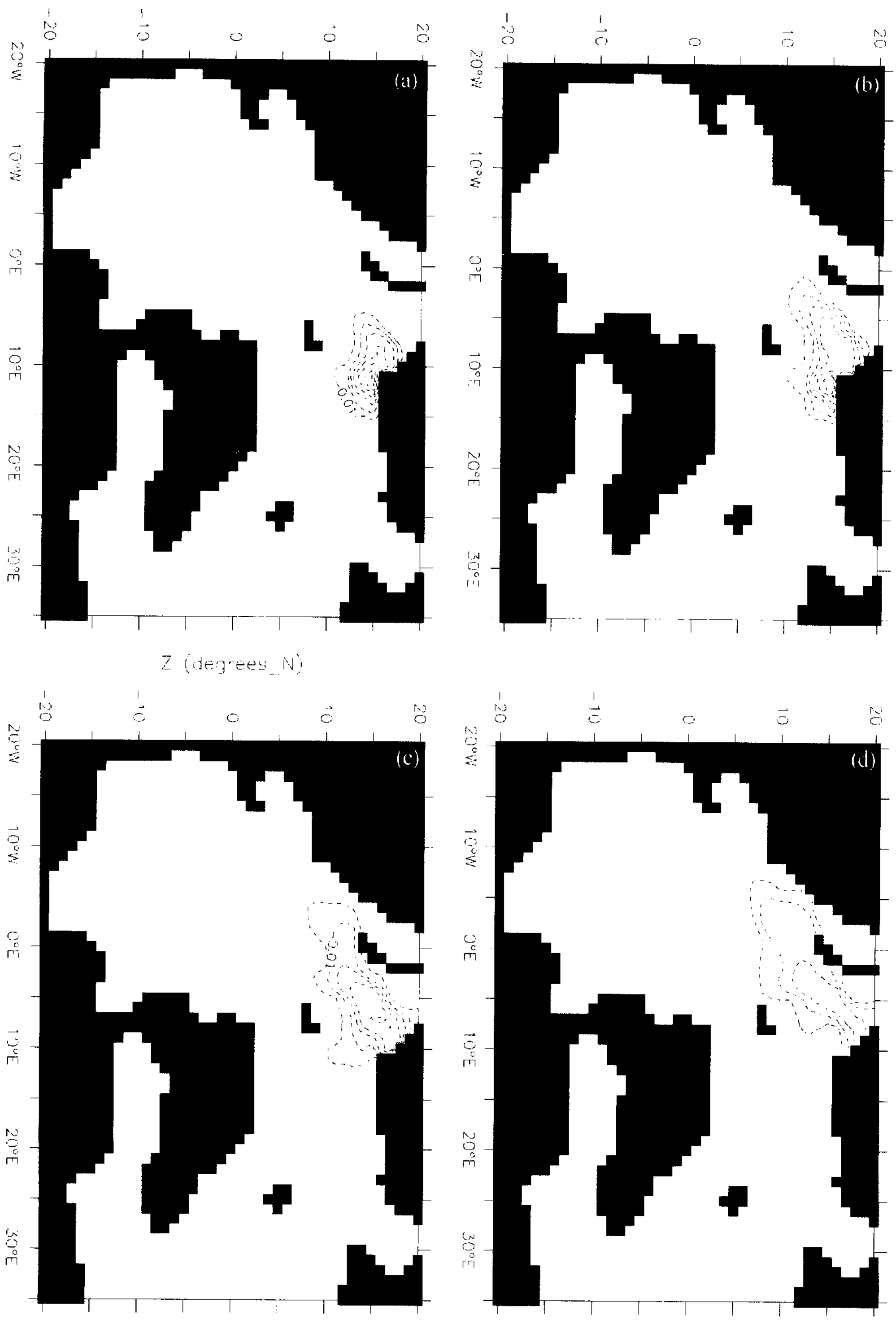

Fig. 2. Winter mean (January through March) surface distribution of the salinity anomaly in experiment A for (a) the last year with anomalous precipitation (= 1998), (b) 1999, (c) 2000, (d) 2001. Contour interval is 0.005. Axis labels refer to the rotated model grid.

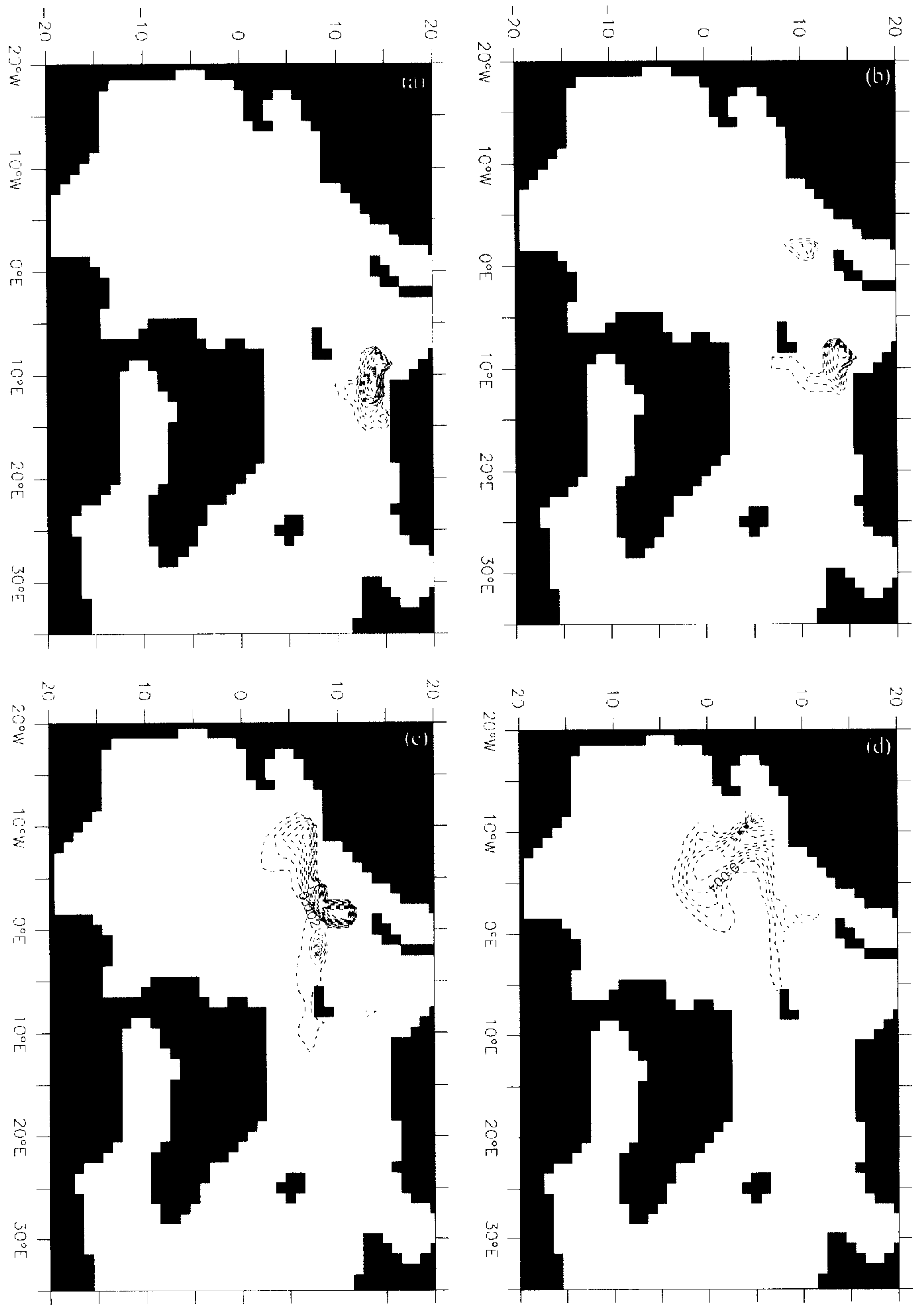

Fig. 3. Winter mean distribution of the salinity anomaly in experiment A at 300 m depth for (a) the last year with anomalous precipitation (= 1998), (b) 2000, (c) 2002, (d) 2005. Contour interval in (a) and (b) is 0.002 and in (c) and (d) is 0.001. Axis labels refer to the rotated model grid.

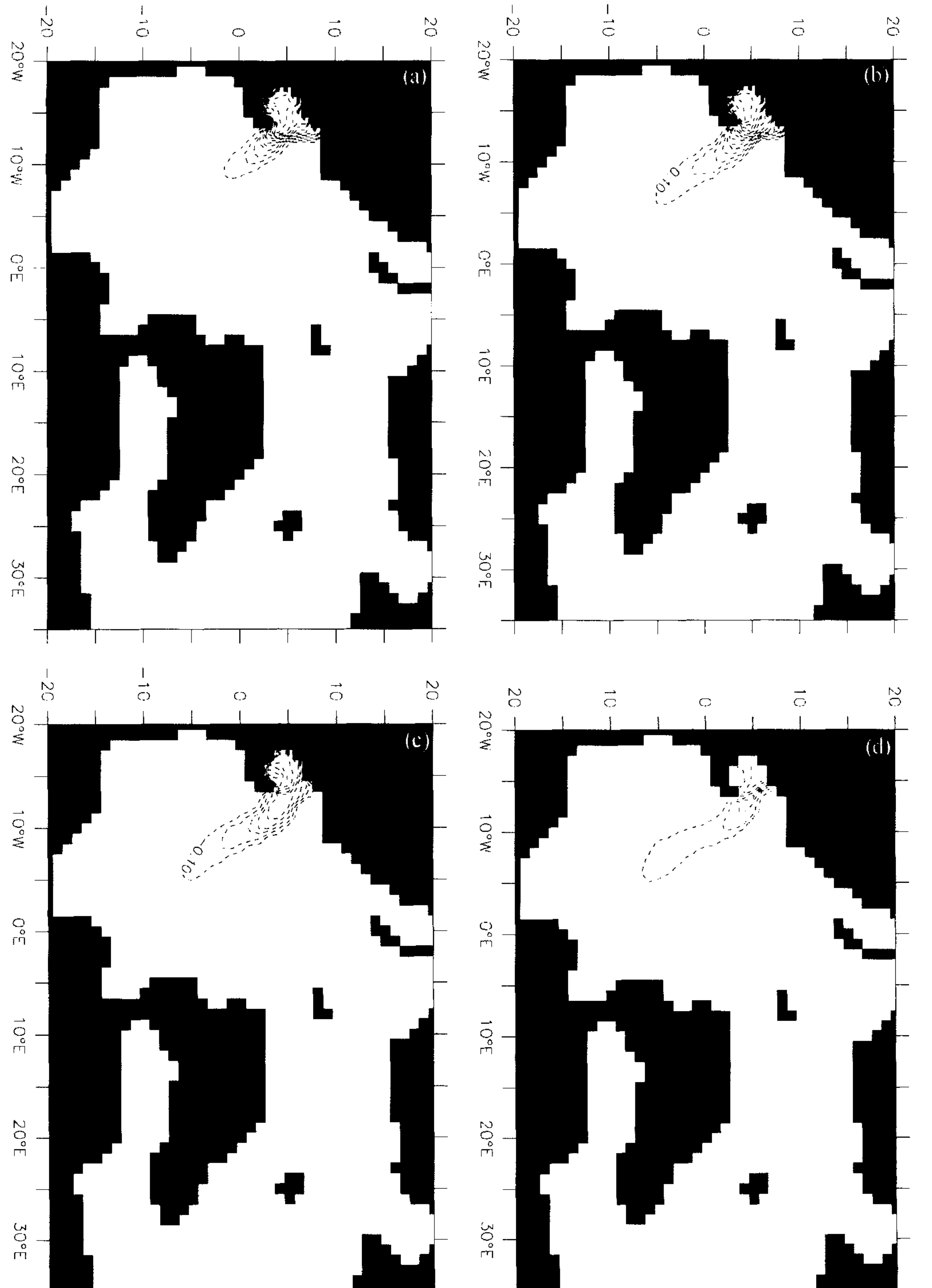

Fig. 4. Winter mean surface distribution of the salinity anomaly in experiment B for (a) the last year with anomalous freshwater flux (= 1998), (b) 1999, (c) 2000, (d) 2001. Contour interval is 0.1. Axis labels refer to the rotated model grid.

anomaly in case B remains at the surface (it is confined to the upper 150 m) and is not transferred to deeper layers. Consequently, the surface density anomaly is much stronger than in case A.

Discussion and conclusion

Surface forcing anomalies selected for our experiments were similar to certain aspects of recent changes in atmospheric forcing and it is appropriate to compare the model results with observations of recent changes in the hydrographic structure of the upper Eurasian Basin. Steele & Boyd (1998) and Schauer, Rudels et al. (unpubl. ms.) describe a retreat of the cold halocline layer from the Amundsen Basin back into the Makarov Basin. This change is attributed to a change in sea ice drift patterns or a diversion of freshwater from the shelves into a more easterly route. Our experiment B indicates that freshwater anomalies that are generated over the Siberian shelf seas by anomalous sea ice formation and/or river run-off can affect the surface salinity along the oceanic transpolar drift. However, the part of the original anomaly that propagates into the interior is small; maximum salinity perturbations in the Makarov Basin are 0.2 psu, one order of magnitude smaller than in the Laptev Sea. Observed changes in the Amundsen Basin are around 0.3 psu (Schauer, Rudels et al. unpubl. ms.). It has to be kept in mind that our response experiment only considers a freshwater flux anomaly and does not take into account the changes in the wind field between negative and positive phases of the NAO or associated with a longer-term trend. Furthermore, the wind forcing used here is biased toward the cyclonic regime of the Arctic Ocean circulation (Proshutinsky & Johnson 1997) because it is based on wind data from the period 1979 to 1993. The effect of wind related changes in oceanic circulation might well be stronger than the freshwater flux anomaly effect in our experiment where the salinity anomaly behaves more or less passively once it has left the Laptev Sea.

Schauer, Rudels et al. (unpubl. ms.) find reduced density between 100 m and 1500 m and reduced salinity between 500 m and 1500 m in the Amundsen Basin when comparing data from 1996 to observations taken five years earlier. A warming signal in the Atlantic layer indicates a stronger contribution of Atlantic Water in that area. However, the salinity changes are too low to compensate the density effect of the temperature as would be expected for just a stronger inflow of Atlantic Water through Fram Strait. Apparently, water mass modifications affecting primarily salinity are necessary to explain the observed changes. These could be melting of sea ice, increased precipitation and run-off. The presence of a salinity anomaly at depth hints at a source of the anomaly located in or upstream of the Barents Sea because water recently in contact with the surface is injected into intermediate depths primarily at the outflow from the Barents Sea at the St. Anna Trough. Results of experiment A show that a precipitation anomaly in the Nordic seas, which is typical for the difference between high and low index phases of the NAO (Dickson et al. in press), can lead to large-scale freshening in the Barents Sea and along the pathway of the Barents Sea branch of the Atlantic inflow into the Arctic. A few years after the anomaly, the freshening occupies a 1000 m thick layer east of the St. Anna Trough and a somewhat shallower layer further along the path towards Fram Strait. This reflects the slower advection speed in the lower layers and it is conceivable that the deep anomaly will reach the central Amundsen Basin a few years after the surface signal. The model results suggest a delay between the forcing in the Nordic/ Barents Sea and the arrival in the central Amundsen Basin of roughly a decade. The salinity anomalies measured at depth in 1996 would thus be the signal of the high NAO fresh water forcing of the late 1980s.

In experiment A we have not included an increased inflow into the Barents Sea due to strengthened circulation in the Nordic Seas. With this we perhaps underestimate the anomaly, as the total forcing is likely to increase the outflow through the St. Anna Trough and feed a stronger boundary current in the Eurasian Basin. Still, with only one process taken into account, the qualitative properties of the simulated salinity anomalies are consistent with recent observations in the Amundsen Basin.

Acknowledgements. – This work was in part funded by the Bundesministerium für Forschung und Technologie through grant 07 VKV01 and by the European Commission Mast III Programme through contract MAS3-CT96-0070 (VEINS). We thank Markus Harder for providing the sea ice model code and Frank Röske for supplying the ECMWF forcing data.

References

Dickson, R. R., Osborn, T. J., Hurrell, J. W., Meincke, J., Blindheim, J., Adlandsvik, B., Vinje, T., Alekseev, G., Maslowski, W. & Cattle, H. in press: The Arctic Ocean response to the North Atlantic Oscillation. *J. Climate.*

Gerdes, R. & Schauer, U. 1997: Large-scale circulation and water mass distribution in the Arctic Ocean from model results and observations. *J. Geophys. Res. 102(C4)*, 8467–8483.

Harder, M. 1997: Roughness, age and drift trajectories of sea ice in large-scale simulations and their use in model verifications. *Ann. Glaciol. 25*, 237–240.

Hibler, W. D. 1979: A dynamic thermodynamic sea ice model. *J. Phys. Oceanogr. 9*, 815–846.

Hibler, W. D. & Bryan, K. 1987: A diagnostic ice-ocean model. *J. Phys. Oceanogr. 7*, 987–1015.

Levitus, S. 1982: *Climatological atlas of the world ocean. NOAA Publ. 13.* 173 pp. Washington, D.C.: US Department of Commerce.

Levitus, S. & Boyer, T. P. 1994a: *World ocean atlas 1994. Vol. 3. Salinity.* 99 pp. Washington, D.C.: National Oceanographic Data Center/US Department of Commerce.

Levitus, S. & Boyer, T. P. 1994b: *World ocean atlas 1994. Vol. 4. Temperature.* 117 pp. Washington, D.C.: National Oceanographic Data Center/US Department of Commerce.

Pacanowski, R. C. 1995: *MOM 2 documentation, user's guide and reference manual. GFDL Ocean Group Technical Report No. 3.* 232 pp. Princeton, NJ: Geophysical Fluid Dynamics Laboratory/Princeton University.

Proshutinsky, A. Y. & Johnson, M. A. 1997: Two circulation regimes of the wind-driven Arctic Ocean. *J. Geophys. Res. 102(C6)*, 12493–12514.

Röske, F. in prep.: Ocean model intercomparison project (OMIP): common forcing and an atlas based on ECMWF reanalysis data. MPI report. Hamburg: Max-Planck-Institut für Meteorologie.

Schauer, U., Muench, R. D., Rudels, B. & Timokhov, L. 1997: Impact of eastern Arctic shelf waters on the Nansen Basin intermediate layers. *J. Geophys. Res. 102*, 3371–3382.

Schauer, U., Rudels, B., Jones, P., Anderson, L. G., Muennich, R. D., Bork, B., Swift, J. H., Ivanov, V. & Larson, A.-M. unpubl. ms.: Water mass distribution in the Eastern Eurasian Basin and connections with the Canadian Basin: results from ACSYS-96.

Steele, M. & Boyd, T. 1998: Retreat of the cold halocline layer in the Arctic Ocean. *J. Geophys. Res. 103(C5)*, 10419–10435.